Available online at www.sciencedirect.com
ScienceDirect
Journal of Photochemistry and Photobiology A: Chemistry 191 (2007) 114–121
Journal of Photochemistry and Photobiology A:Chemistry
www.elsevier.com/locate/jphotochem

Spectral and kinetic properties of a red–blue pH-sensitive photochromic spirooxazine

E.B. Gaeva [a], V. Pimienta [b], S. Delbaere [c], A.V. Metelitsa [a], N.A. Voloshin [a], V.I. Minkin [a], G. Vermeersch [c], J.C. Micheau [b,*]

[a] *Institute of Physical Organic Chemistry, Southern Federal University, Rostov on Don, Russia*
[b] *IMRCP, UMR CNRS 5623, Université P. Sabatier, F-31062 Toulouse, France*
[c] *UMR CNRS 8009, Université de Lille 2, Faculte de Pharmacie, F-59006 Lille Cedex, France*

Received 21 February 2007; received in revised form 3 April 2007; accepted 6 April 2007
Available online 13 April 2007

Abstract

By means of UV/Vis absorption spectroscopy, NMR measurements and kinetic modelling, two spironaphthoxazine compounds bearing 5-OAlk substituent have been investigated in neutral and acidified ethanol media. The kinetics of ring opening/ring closure and the equilibrium constant, the quantum yield of photocoloration, the molar absorption coefficients of the neutral and protonated open forms and pK_a values have been determined. A three-species photoreversible transformation between the closed form, the open form and the protonated open form has been observed in slightly acidified solutions.
© 2007 Elsevier B.V. All rights reserved.

Keywords: Spironaphthoxazine; Photochromism; Acidichromism; Molecular switch; Kinetic modelling

1. Introduction

The discovery of the remarkable fatigue resistance of photochromic spirooxazines has opened vast perspectives for their potential practical applications [1,2]. One of the essential features of these photochromic compounds is the relatively low thermal stability of UV-photoinduced merocyanine isomer [3,4]. Under continuous irradiation, the system reaches a coloured photo-steady-state of variable intensity. This property is attractive for regulating light fluxes but inhibitory for potential use in permanent optical memories. Further investigations are then needed to find experimental situations where the merocyanine is stabilised. For instance, avoiding the spontaneous back-reaction of the open merocyanine towards the closed spiroform could give rise to systems possibly mimicking logic gate or data recording behaviour [5–7]. The pH effects were found to be very interesting to stabilise the open merocyanine by inhibiting the thermal ring closure, but letting the system to be bleached by visible light irradiation. The possibility to switch between the various forms and thus the various properties by turning the UV light on and off and adjusting the pH value make spirooxazines very versatile compounds.

The present work was aimed at the determination of the quantitative characteristics of the photoinduced and thermal reactions of the substituted spironaphthoxazines **1**–**2** in neutral and acidic organic media.

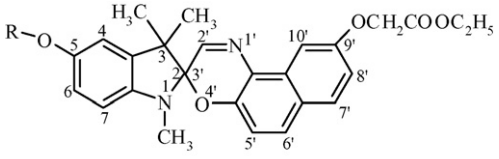

R – **1**: CH_3; **2**: C_9H_{19};

These compounds are characterised by the presence of a donor –O–alkyl substituent with variable carbon chain lengths in the 5-position of the indoline part and by a $–O–CH_2–COOC_2H_5$ group on the 9′-position of the naphthoxazine part.

The purpose of this paper is to combine UV/Vis, NMR and kinetic measurements to determine the molar absorption coefficient of the thermally unstable open merocyanine form, the rate constants of ring opening and ring closure and the corresponding equilibrium constant between the open and closed forms.

* Corresponding author. Tel.: +33 5 61 55 62 75; fax: +33 5 61 55 81 55.
E-mail address: micheau@chimie.ups-tlse.fr (J.C. Micheau).

1010-6030/$ – see front matter © 2007 Elsevier B.V. All rights reserved.
doi:10.1016/j.jphotochem.2007.04.011

On the other side, the determination of quantum yields of the UV-induced ring opening, the pK_a of the open merocyanine and the molar absorption coefficient of the protonated open form will require kinetic analysis [8–11] of Abs versus time curves recorded under monochromatic continuous irradiation or after protonation.

2. Experimental

The synthesis of ethyl 5-methoxy-l,3,3-trimethylspiro-[indoline-2,3′-[3H]naphtho[2,l-b][l,4]oxazine]-9′-yloxyacetate **1** and ethyl 5-nonyloxy-l,3,3-trimethylspiro-[indoline-2,3′-[3H]naphtho[2,l-b][l,4]oxazine]-9′-yloxyacetate **2** was thoroughly described previously [12]. Solvents for UV/Vis spectroscopy (acetonitrile, ethanol, cyclohexane and toluene) were of the highest spectroscopic grade (Acros Organics). Concentrated hydrochloric and sulphuric acids were of the analytical grade and were used without any further purification.

2.1. Photokinetic experiments

Absorption spectra and photokinetic data (absorbance versus time matrices) were recorded on a thermostated Ocean Optic diode array fiber optic spectrophotometer. The photochromic solution (2 mL) was stirred continuously with a magnetic bar driven by a variable-speed stepper motor in the 1 cm × 1 cm quartz cell closed with a Teflon bung. The whole setup was enclosed in a thermostatic block. Otherwise specified, all the experiments were conducted at 27 °C (300 K). The irradiation was derived from a 200 W high-pressure mercury lamp equipped with interference filters enabling transmission of a selected single emission line. The monochromatic light intensity was determined directly in the reactor using an aqueous solution of potassium ferrioxalate. The stability of the photon flux was checked by a semiconductor photosensor before and after each experiment ($I_o^{313} = 2.4 \times 10^{-6}$ mol L^{-1} s^{-1}; $I_o^{365} = 3.1 \times 10^{-6}$ mol L^{-1} s^{-1}). The data were stored and processed on a desk PC computer using homemade software in order to obtain experimental photokinetic curves ($Abs_{exp}(\lambda)$ versus t).

Assumed mechanism was translated into a series of kinetic differential equations involving the concentrations of all the species. Beer's law was then used to calculate the values of the absorbances. The calculated $Abs_{calc}(\lambda)$ versus t curves were obtained by numerical integration using a Runge–Kutta semi-implicit procedure. In order to check the validity of the model and to estimate the required parameters, the residual error (RE): $RE = \Sigma_p \Sigma_j [Abs_{calc}(j) - Abs_{exp}(j)]^2 / pj$, where p is the number of plots fitted simultaneously and j is the number of points in each plot, was minimized until a good fit was reached. The minimization algorithm is of the Powell type. The set of optimized parameters was checked to be unique.

2.2. UV/Vis-NMR combined experiment

NMR experiments were carried out in methanol-d_4 and were recorded on Bruker spectrometers (^{1}H, 500 MHz or 300 MHz) using standard sequences.

Photoirradiation was carried out directly into the NMR tube in a home-built apparatus with a 1000 W high-pressure Hg–Xe lamp equipped with filters. Monochromic UV light was obtained by passing the light through a first filter (Schott 11FG09: $259 < \lambda < 388$ nm with $\lambda_{max} = 330$ nm, $T = 79\%$), then through an interferential one ($\lambda = 313$ nm and $T = 7\%$).

For UV–visible measurements, a fibre optic micro volume probe (C Technologies Inc., optical path: 2 mm, Length: 180 mm, Diameter: 3 mm) coupled with a Cary 50 UV–vis spectrometer (Varian) is immersed into the NMR tube.

NMR and UV–visible spectra of the same sample are recorded before and after irradiation. From NMR data, concentrations are deduced, from UV spectra, molar absorption coefficients can be calculated.

2.3. Determination of the relative proportions of *A*, *B* and *BH*$^+$ of spirooxazine *1* by UV/Visible spectroscopy

From Beer's law at any wavelength X we have: $Abs^\lambda = (\varepsilon_A^\lambda[\mathbf{A}] + \varepsilon_B^\lambda[\mathbf{B}] + \varepsilon_{BH+}^\lambda[\mathbf{BH^+}])\, l_{opt}$. By selecting two wavelengths λ_1 and λ_2 in the visible region where A does not absorb ($\varepsilon_A^\lambda = 0$), the following equations can be derived:

$$[\mathbf{B}] = \frac{(\varepsilon_{BH+}^{\lambda 1} Abs^{\lambda 2} - \varepsilon_{BH+}^{\lambda 2} Abs^{\lambda 1})}{[(\varepsilon_{BH+}^{\lambda 1}\varepsilon_B^{\lambda 2} - \varepsilon_B^{\lambda 1}\varepsilon_{BH+}^{\lambda 2}) l_{opt}]}$$

$$[\mathbf{BH^+}] = \frac{(\varepsilon_B^{\lambda 2} Abs^{\lambda 1} - \varepsilon_B^{\lambda 1} Abs^{\lambda 2})}{[(\varepsilon_{BH+}^{\lambda 1}\varepsilon_B^{\lambda 2} - \varepsilon_B^{\lambda 1}\varepsilon_{BH+}^{\lambda 2}) l_{opt}]}$$

Values of the molar absorption coefficients taken from Tables 2 and 4 and Fig. 3 and $\lambda_1 = 532$ nm, $\lambda_2 = 621$ nm have been used. For SPO **1**, the following values have been used: $\varepsilon_{BH+}^{532} = 23200$; $\varepsilon_{BH+}^{621} = 2300$; $\varepsilon_B^{532} = 9400$; $\varepsilon_B^{621} = 32500$ L mol^{-1} cm^{-1}; $l_{opt} = 1$ cm. Then $[\mathbf{A}] = [\mathbf{A}]_o - [\mathbf{B}] - [\mathbf{BH^+}]$, where $[\mathbf{A}]_o$ is the initial concentration of the spirooxazine.

3. Results and discussion

3.1. UV-induced ring opening and thermal back-reaction

3.1.1. UV–visible spectroscopic analysis

In solutions, 9′-ethyloxyacetate substituted spiro[indole-2,3′-naphtho[2,l-b]oxazines **1–2** appear mainly as the cyclic form **A**. Nevertheless, a light blue colour related to the presence of a small amount of merocyanine open form **B** in thermal equilibrium with the cyclic form **A** ($K_{eq} = [\mathbf{B}]/[\mathbf{A}] \ll 1$) can be observed in spirooxazine (SPO) solutions at concentration around 10^{-3} mol L^{-1}. In different solvents (cyclohexane, toluene, acetonitrile, ethanol) the cyclic forms **A** of spirooxazines of naphthalene series are characterized by an absorption band around 322–327 nm ($\varepsilon^{max} \approx 8500$–$9800$ L mol cm^{-1}). UV irradiation leads to the formation of the merocyanine open forms B exhibiting an intense absorption band between 572 and 621 nm depending on the solvent polarity. Table 1 shows the UV/Vis spectral characteristics (λ_A^{max} and ε_A^{max}) of the closed form **A**, but only λ_B^{max} of the open form **B** because calculation of the

Table 1
Maximal absorption wavelengths and molar absorption coefficients of the spiro-form (**A**) and photomerocyanine (**B**) in different solvents

Compound	Solvent	λ_A^{max} (nm)	ε_A^{max} (L mol^{-1} cm^{-1})	λ_B^{max} (nm)
1	Cyclohexane	326	8500	572
	Toluene	327	9000	607
	Acetonitrile	323	8900	611
	Ethanol	323	9400	621
2	Cyclohexane	322	9800	583
	Toluene	324	9100	611
	Acetonitrile	323	9300	613
	Ethanol	323	9600	621

The solvents have been sorted from top to bottom according to decreasing Brooker's X_R solvatochromic parameters [13].

molar absorption coefficient of **B** requires the determination of its concentration [**B**] (see Section 3.1.2).

The regular increase of the λ_B^{max} for cyclohexane, toluene, acetonitrile and ethanol is consistent with the zwitterionic character of the merocyanine **B** [14]. A chain length effect is only seen in the less polar solvent (cyclohexane). For intermediate solvents, toluene and acetonitrile, this bathochromic effect is slightly visible going from CH_3 to C_9H_{19}. No variation is evidenced in ethanol. Under continuous UV irradiation, the photochromic systems reach a photosteady state. While acetonitrile, toluene and cyclohexane give rise to moderately intense merocyanine absorption, alcohols induce a significantly more intense band. Hence, ethanol or methanol were selected as preferential solvent for further studies. Thermal ring closure from **B** to **A** occurs in the dark and this bleaching kinetic is not accelerated by an intense green light irradiation at 546 nm.

All these experimental results suggest that the spiro and the merocyanine forms are coupled by two thermal (k_{AB} and k_{BA}) and one photochemical (Φ_{AB}) isomerisation processes.

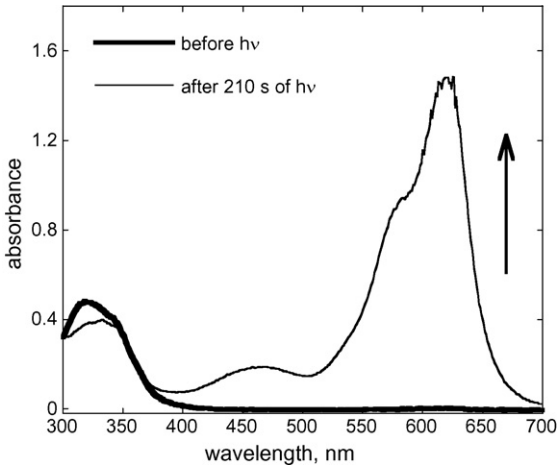

Fig. 2. UV/visible absorption spectra of SPO **2** in CD_3OD at 243 K before and after 210 s irradiation with $\lambda = 313$ nm. $[SPO]_0 = 3.5 \times 10^{-4}$ mol L^{-1}; $l_{opt} = 0.2$ cm.

3.1.2. Determination of the molar absorption coefficient of the merocyanine open form B

The molar absorption coefficients of merocyanines **1**–**2** have been obtained by combining ^{1}H NMR spectroscopy with UV/Vis spectrophotometry measurements after low temperature UV irradiation. This method enables the **A** ⇆ **B** equilibrium to be substantially shifted towards the open merocyanine **B** which, otherwise, would not be detectable by ^{1}H NMR technique in the dark and at room temperature. Fig. 1 shows details of the ^{1}H NMR spectra of compound **2** before and after 210 s of UV irradiation and Fig. 2 displays the corresponding evolution of the UV/visible absorption of the UV irradiated NMR tube.

The average concentrations of the cyclic and open forms were determined by ^{1}H NMR spectrometry while the corre-

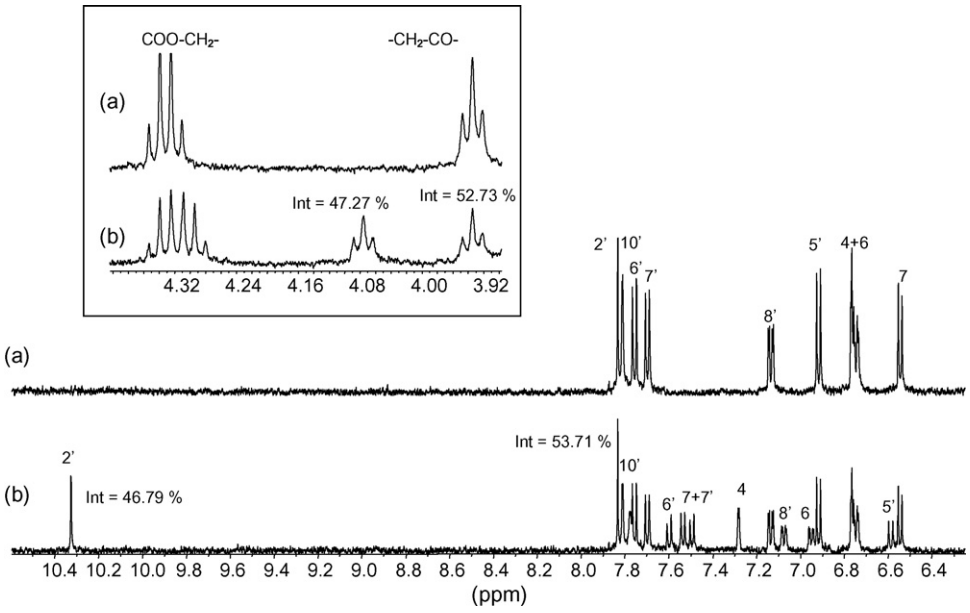

Fig. 1. ^{1}H NMR part of spectra (a) before and (b) after 210 s under irradiation with $\lambda = 313$ nm of SPO **2** in CD_3OD (3.5×10^{-4} mol L^{-1}) at 243 K. (insert: aliphatic protons between 3.90 and 4.40 ppm). $r = [\mathbf{B}]/[\mathbf{A}] = 0.88 \pm 0.015$.

Table 2
Molar absorption coefficients of photomerocyanines **B** of spirooxazines **1–2**

Compouds	Concentration of [**B**]	Abs	Epsilon L mol^{-1} cm^{-1} (621 nm)
SPO **1** (CH_3)	2.12×10^{-4} M	1.378	32500 ± 2000
SPO **2** (C_9H_{19})	1.64×10^{-4} M	1.409	42800 ± 4000

(l_{opt} = 0.2 cm).

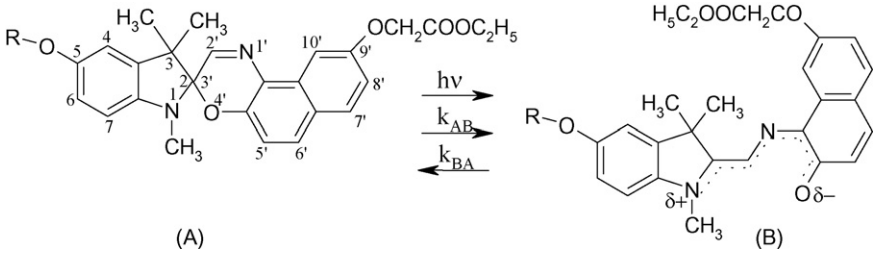

Scheme 1. Assumed photochromic mechanism of compounds **1–2** in alcoholic solution.

A + hν →**B** (Φ_{AB})	$v_1 = \Phi_{AB} I'_0 \varepsilon'_A[\mathbf{A}]F'$	[1]
A→**B** (k_{AB})	$v_2 = k_{AB}[\mathbf{A}]$	[2]
B →**A** (k_{BA})	$v_3 = k_{BA}[\mathbf{B}]$	[3]

Scheme 2. Kinetic model of the photochromic mechanism.

sponding absorbance values were provided by the UV/Visible measurements. Molar ratio [**B**]/[**A**] is equal to the NMR proton integration ratio r. Then, $[\mathbf{B}] = r[\mathbf{A}]_0/(1+r)$ and $\varepsilon_B = Abs/[\mathbf{B}]l_{opt}$). Molar absorption coefficients of the photomerocyanine **B** for compounds **1–2** are gathered in Table 2.

3.1.3. Kinetic modelling of the photochromic mechanism

The photochromic mechanism shown in Scheme 1 can be summarized by the following kinetic model (Scheme 2) which depicts three main isomerization processes: two forward isomerizations from **A** to **B**, the first is photochemical with a quantum yield Φ_{AB}, the second is thermal with a first order rate constant: k_{BA}; the third process is the thermal back reversion (k_{BA}) from **B** to **A**.:

where $I_o^{'}$ is the incident monochromatic photon flux at irradiation wavelength λ′ (moles of photons L^{-1} s^{-1}); $\varepsilon_A^{'}$ is the molar absorption coefficient of the cyclic form **A** at the irradiation wavelength λ′ (L mol^{-1}); F is the adimensional photokinetic factor, $F = (1 - 10^{-Abs'})/Abs'$; v_i is the rate of process i (mol L^{-1} S^{-1}). Optical path is 1 cm.

3.1.4. Φ_{AB} determination

From the kinetic model shown on Scheme 2, the following equations can be written:

- the evolution of [**A**]:

$$\frac{d[\mathbf{A}]}{dt} = -v_1 - v_2 + v_3 = [\mathbf{A}]((\Phi_{AB} I'_o \varepsilon'_A F' + k_{AB}) + k_{BA}[\mathbf{B}] \quad (1)$$

- the mass balance equation:

$$[\mathbf{A}] + [\mathbf{B}] = [\mathbf{A}]_0 \quad (2)$$

- and the Beer's law:

$$Abs^{\lambda} = (\varepsilon_A^{\lambda}[\mathbf{A}] + \varepsilon_B^{\lambda}[\mathbf{B}])l_{opt} \quad (3)$$

Fig. 3 (left) shows the thermal relaxation in the dark recorded after switching-off the UV irradiation. Mono-exponential behaviour is in agreement with our mechanistic hypothesis with an apparent rate constant $k_{obs} = k_{AB} + k_{BA}$. Fig. 3 (right)

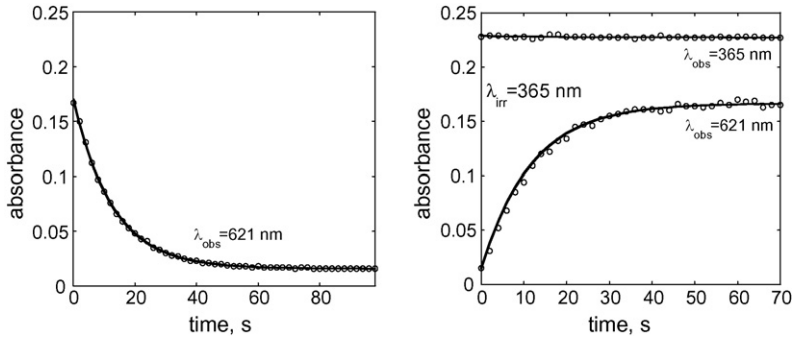

Fig. 3. Kinetics analysis of the photochromism of a 6.22×10^{-5} mol L^{-1} solution of SPO **1** in ethanol at 300 K. (left): thermal relaxation after switching-off of the UV irradiation; (right): monitoring of 621 and 365 nm under continuous monochromatic irradiation at 365 nm. Dots are experimental data, continuous lines are numerical fittings.

Table 3
Extracted photokinetic and thermodynamic parameters of spiro[naphthoxazines] **1–2** in ethanol solution at 300 K

Kinetic and thermodynamic parameters	**1**	**2**
k_{obs} (S^{-1})	7.32×10^{-2}	7.44×10^{-2}
k_{AB} (S^{-1})	2×10^{-4}	1.7×10^{-4}
k_{BA} (S^{-1})	7.30×10^{-2}	7.42×10^{-2}
Φ_{AB}	0.3 ± 0.05	0.3 ± 0.05
K_{eq}	2.7×10^{-3}	2.3×10^{-3}
ΔG^0 (kJ mol^{-1})	13.2	13.6

illustrates the two wavelengths fitting of Abs^{λ} versus time photokinetic curves recorded under continuous irradiation. For the sake of clarity, only the kinetics under 365 nm irradiation are exhibited. Note that Abs^{365} remains constant due to the presence of an isosbestic point [15] at this wavelength. Irradiation at 313 nm (not shown) gives similar results as 313 nm is a second isosbestic point. As it is shown, the proposed mechanism reproduces the experimental points satisfactorily.

Extracted isomerisation rate constants and photocoloration quantum yield for SPO **1–2** are gathered in Table 3.

From the equilibrium constants $K_{eq} = [\mathbf{B}]/[\mathbf{A}] = k_{AB}/k_{BA}$, the standard free energy difference between the open and closed isomers can be estimated using the equation $\Delta G^0 = -RT \ln K_{eq}$. The open forms **B** is more energetic than the closed one by about 13–14 kJ mol^{-1}. These results also show that the carbon chain length has little influence on the photochromic parameters of the spirooxazines **1** and **2**. A tiny effect can however be seen on the k_{AB} thermal ring opening rate constant, which slightly decreases going from CH_3 to C_9H_{19}, possible steric hindrance could be involved.

3.2. Spectral and thermodynamic properties in acid medium

3.2.1. Protonation of spirooxazines

When an ethanol solution of spirooxazines **1–2** is acidified, the solution stains progressively red. A gaussian-shaped absorption band appears with a maximum at about 532 nm (Fig. 4a).

When an equivalent of base is added to the acidified solution, the absorbance at $\lambda_{max} = 532$ nm is rapidly replaced by the absorbance at $\lambda_{max} = 621$ nm i.e. by the spectrum of the blue non-protonated merocyanine (Fig. 4b). This transformation is followed by a slow thermal bleaching (Fig. 4b–e). This result confirms the reversibility of the protonation–deprotonation of the open merocyanine **B**. Owing to the zwitterionic structure of the open merocyanine form, it is likely that the protonation is realized at the oxygen atom [16] (Scheme 3).

When the concentration of hydrochloric acid is comparable to the concentration of the spironaphthoxazine, the acidified solution keeps its colour for several days. This effect can be interpreted by the coupling between the closed/open equilibrium $\mathbf{A} \leftrightarrows \mathbf{B}$ and the protonation equilibrium $\mathbf{B} + \mathbf{H}^+ \leftrightarrows \mathbf{BH}^+$. Depending of the relative values of the equilibrium constants and of the concentrations, there is a stabilization of the coloured

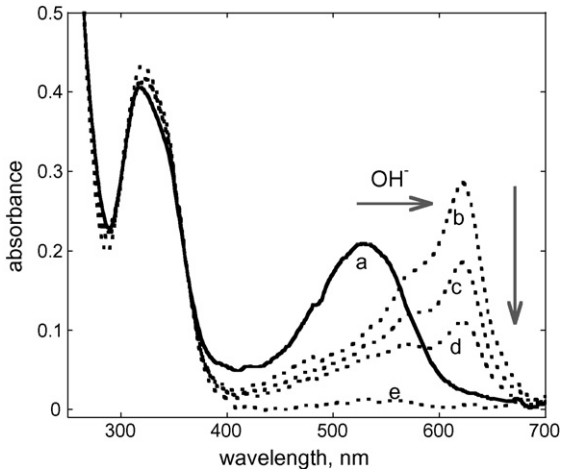

Fig. 4. Visible absorption of an acidified ethanol solution of **1** (6.3×10^{-5} mol L^{-1}) (a: 3000 s after 1 equivalent HCl addition) and spectral evolution after 1 equivalent NaOH addition (b: 8; c: 20; d: 36; e: 80 s).

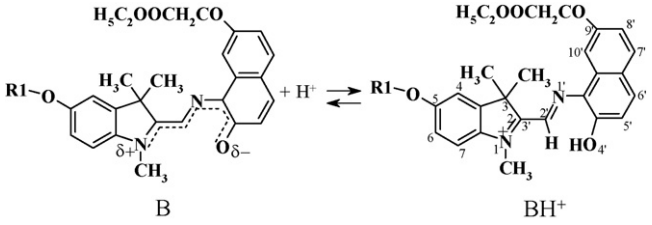

Scheme 3. Reversible protonation of the merocyanine open form.

A→B (k_{AB})	$v_2 = k_{AB}[A]$	[2]
B→A (k_{BA})	$v_3 = k_{BA}[B]$	[3]
$\mathbf{B} + \mathbf{H}^+ \rightarrow \mathbf{BH}^+$	$v_4 = k_3[B][H^+]$	[4]
$\mathbf{BH}^+ \rightarrow \mathbf{B} + \mathbf{H}^+$	$v_5 = k_4[BH^+]$	[5]

Scheme 4. Kinetic model of the acidichromism.

open form by the formation of a protonated merocyanine [17,18]. This property is known as acidichromism [19–24]. A mechanism accounting for the processes that occur after acid addition into an ethanol solution of a spirooxazine **1–2** can be schematized in Scheme 4.

The first and the second processes [2] and [3] correspond to thermal equilibrium between the closed spiro **A** and the open merocyanine form **B**. The third and the forth ones [4] and [5] illustrate the merocyanine protonation equilibrium. The following differential equations have been derived and were applied to the curve fitting process:

$$\frac{dA}{dt} = -v_2 + v_3 \quad (4)$$

$$\frac{dB}{dt} = -v_2 + v_3 - v_4 + v_5 \quad (5)$$

$$\frac{dBH^+}{dt} = v_4 + v_5 \quad (6)$$

$$\frac{dH^+}{dt} = -v_4 + v_5 \quad (7)$$

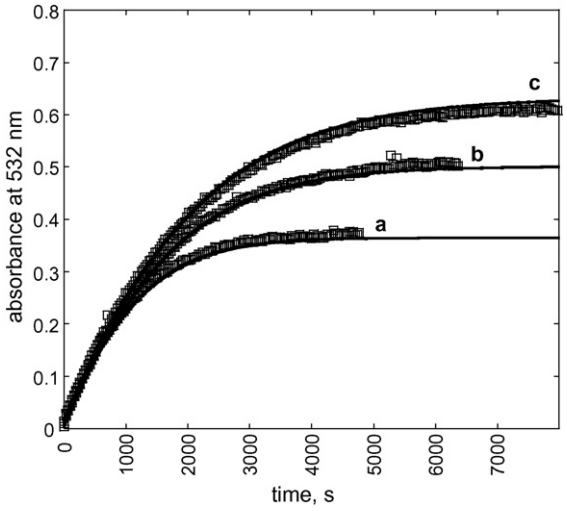

Fig. 5. Kinetic analysis at 300 K of the protonation curves of SPO **2** (1.0×10^{-4} mol L^{-1}) in ethanol solutions at various acid concentrations. [HCl]/[SPO] = a: 1/2; b:3/4; c: 1/1; Squares are experimental data and continuous line are the numerical fittings by the proposed model.

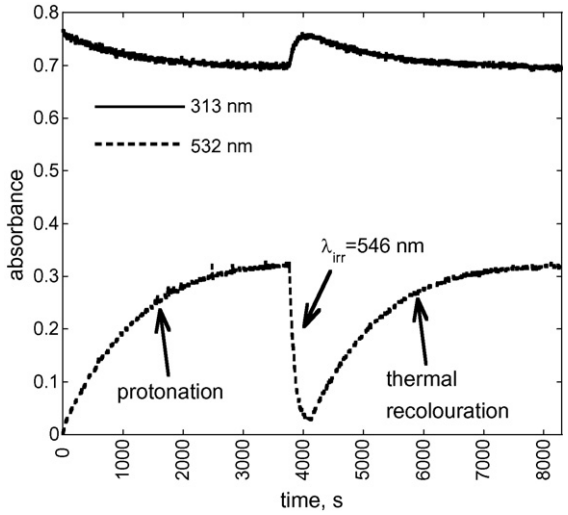

Fig. 6. Negative photochromism of **2** in acidified ethanol solution under visible light irradiation at 546 nm. Note the exact shape of the protonation and thermal re-coloration kinetics. [**2**] = 8×10^{-5} mol L^{-1}; [HCl] = 6.0×10^{-5} mol L^{-1}. T = 300 K.

The colouration kinetics depend on the acid concentration. The colouration kinetic curves recorded after acid injections at following mol/mol proportions [HCl]/[SPO]: 1/2; 3/4 and 1/1 are gathered on Fig. 5.

When the proton concentration increases, the equilibrium concentration of the protonated form increases, while the initial rate remains constant. The two spironaphthoxazines **1** and **2** behave similarly. The main spectral and thermodynamic characteristics such as the molar absorption coefficients of the protonated merocyanine form and their pK_a values have been determined from the numerical modelling of the Abs versus time kinetic curves recorded after protonation. The three curves are fitted simultaneously. Results are reported on Table 4.

The extracted molar absorption coefficients are of the same order of magnitude as those previously reported for unsubstituted spironaphthoxazine ($13{,}400 \pm 400$ L cm^{-1} mol^{-1})[24].

Compared to the non-protonated ones, it appears that for the longer chain spirooxazine **2**, protonation reduces the molar absorption coefficient by a factor higher than two, an effect likely to be due to a loss of conjugation after protonation. This effect is less pronounced for the O-Me substituted SPO **1**. This loss of conjugation is also in agreement with the hypsochromic shift of the merocyanine band under protonation.

If the acid concentration is increased until 10^{-1} mol L^{-1} (i.e. 10^3 times the stoechiometric ratio [H$^+$]/[**A**]$_0$), a degradation accompanied by colour fading slowly occurs with the formation of fluorescent products whose exact structure has not been determined in the present work.

Table 4
pK_a and molar absorption coefficients of the protonated merocyanines of the spironaphthoxazines **1**–**2**

	1	**2**
$K_a = k_4/k_3$	$(6.41 \pm 0.64) \times 10^{-7}$	$(2.49 \pm 0.25) \times 10^{-7}$
pK_a	6.19 ± 0.05	6.60 ± 0.04
ε_{BH+} (L cm^{-1} mol^{-1})	23200 ± 500	16400 ± 500

3.2.2. Negative photochromism

Another interesting phenomenon that has been observed in acidified solutions of SPO **1**–**2** is the negative photochromism of protonated merocyanine. Under irradiation with green light (546 nm) of an acidified SPO solution, an almost complete and fast photobleaching has been observed (Fig. 6).

Visible light irradiation converts more than 90% of the protonated form **BH**$^+$ into the spiro form **A** without any noticeable accumulation of the non-protonated open form **B**. The similitude of the two relaxation kinetic curves (protonation and thermal recoloration) confirms this result suggesting that the protonated merocyanine undergoes direct rearrangement to the spiro form **A**. It is presumed that during this negative photochromic process a proton release takes place: $\mathbf{BH^+} + h\nu\mathbf{(Vis.)} \rightarrow \mathbf{A} + \mathbf{H^+}$.

The presence of UV-induced photochromism, thermal bleaching, acidichromism and visible light induced negative photochromism gives rise to a 3-species photochromic system.

3.3. A three-species photochromic system

The colorless spirooxazine state **A** isomerizes to the blue merocyanine form **B** upon UV irradiation. During this process the appearance of a band at 621 nm is observed. The photogenerated base **B** converts to the purple protonated merocyanine form **BH**$^+$ after the addition of an acid. The absorption band of **B** at 621 nm instantaneously disappears and a new band corresponding to **BH**$^+$ arises at 532 nm. Upon irradiation with green light, the form **BH**$^+$ reverts almost completely back to the spiroform **A** releasing **H**$^+$ (Scheme 5). Therefore, the light and proton actions may be exploited to modulate the switching between the three species **A**, **B** and **BH**$^+$.

At low acid concentrations ([H$^+$] < [SPO]), the relative proportions of the spiroform **A**, the merocyanine **B** and the

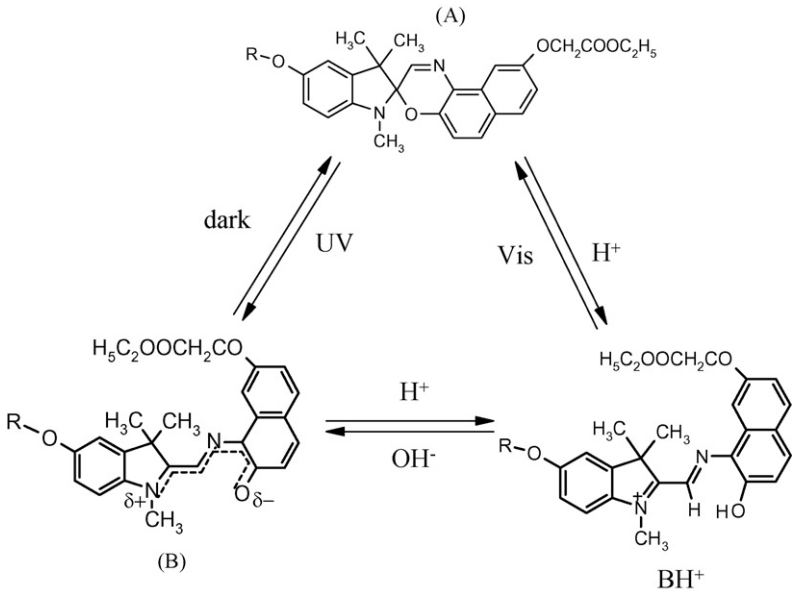

Scheme 5. The reversible interconversion between the three species of spironaphthoxazines. **A**: colorless; **B**: 621 nm; **BH**$^+$: 532 nm.

Table 5
Variation of the relative proportions of the three species **A**, **B** and **BH**$^+$ in various protonated ethanol solutions of SPO **1**

[HCl]/[SPO 1]	%A (hv)	%B (hv)	%BH$^+$(hv)	%A (dark)	%B (dark)	%BH$^+$(dark)
0:1	89	11	0	99.7	0.3	0
1:2	70	7	23	78	0	22
3:4	42	6	52	70	0	30
1:1	22	3	75	62	0	38

[**1**] = 5.91×10^{-5} mol L^{-1} at 300 K under 313 nm irradiation (photosteady state) and in the dark.

protonated merocyanine **BH**$^+$ can be varied significantly by UV irradiation. Table 5 shows the variable proportions of the three species that have been obtained at photosteady state under 313 nm continuous irradiation and in the dark.

These results show that acidification and UV irradiation can be used independently for ring opening. For instance, the same proportion of open form (**B** + **BH**$^+$) can be obtained either under UV irradiation at moderate acidity (1:2) or in the dark but with a higher acid ratio (3:4).

4. Conclusion

The complete study of spironaphthoxazines in neutral and acid ethanol medium under irradiation with UV and visible light has been performed. It is possible to stabilize the open form under protonated merocyanine that stays stable for several days or weeks. A reversible transformation between the spiroform **A**, the merocyanine form **B** and the protonated merocyanine **BH**$^+$ can be realized by adjusting the irradiation light and pH value. For the first time, all the photokinetic characteristics of spirooxazines 1 and 2 have been determined. It has been shown that increasing the chain length increases the conjugation of the non-protonated merocyanines while conjugation of the protonated forms are, on the contrary, decreased. On the other hand, photocolouration quantum yields remain unaffected.

The possibility to switch between the various forms and thus the various properties by turning the UV light on and off and adjusting the pH makes the spirooxazines very interesting for potential practical purposes. Such systems are able to modulate their response as a function of several external inputs. Due to the simultaneous presence of positive (under UV) and negative (under visible light) photochromism they could operate as mimics for logic gates behaviour.

References

[1] N.Y.C. Chu, Can. J. Chem. 61 (1983) 300–305.
[2] V. Lokshin, A. Samat, A.V. Metelitsa, Russ. Chem. Rev. 71 (2002) 893–917.
[3] N.Y.C. Chu, Photochromism, in: H. Dürr, H. Bouas-Laurent (Eds.), Molecules and Systems, vol.10, Elsevier, Amsterdam, 1990, p. 493.
[4] R.C. Bertelson, in: G.H. Brown (Ed.), Photochromism, Wiley-Inter science, New York, 1971, p. 45.
[5] H. Choi, B.S. Ku, S.R. Keum, S.O. Kang, J. Ko, Tetrahedron 61 (2005) 3719–3723.
[6] S. Giordani, M.A. Cejas, F.M. Raymo, Tetrahedron 60 (2004) 10973–10981.
[7] X. Guo, D. Zhang, D. Zhu, Adv. Mater. 61 (2004) 125–130.
[8] F. Wilkinson, J. Hobley, M. Naftaly, J. Chem. Soc, Faraday Trans. 88 (1992) 1511–1517.
[9] V. Pimienta, D. Lavabre, G. Levy, A. Samat, R. Guglielmetti, J.C. Micheau, J. Phys. Chem. 100 (1996) 4485–4490.
[10] M.H. Deniel, J. Tixier, B. Houzé-Luccioni, D. Lavabre, J.C. Micheau, Mol. Cryst. Liq. Cryst. 298 (1997) 121–128.
[11] V. Pimienta, J.C. Micheau, Mol. Cryst. Liq. Cryst. 344 (2000) 157–162.

[12] N.A. Voloshin, A.V. Metelitsa, J.C. Micheau, E.N. Voloshina, S.O. Besugliy, A.V. Vdovenko, N.E. Shelepin, V.I. Minkin, Russ. Chem. Bull. Int. Ed. 52 (2003) 1172–1181.
[13] L.G.S. Brooker, A.C. Craig, D.W. Heseltine, P.W. Jenkins, L.L. Lincoln, J. Am. Chem. Soc. 87 (1965) 2443–2450.
[14] A.V. Metelitsa, V. Lokshin, J.C. Micheau, A. Samat, R. Guglielmetti, V.I. Minkin, Phys. Chem. Chem. Phys. 4 (2002) 4340–4345.
[15] M.H. Deniel, D. Lavabre, J.C. Micheau, in: J.C. Crano, R.J. Guglielmetti (Eds.), Organic Photochromic and Thermochromic Compounds, vol. 2, Kluwer Academic/Plenum Publishers, New York, 1999, p. 172.
[16] P. Rys, R. Weber, Q. Wu, Can. J. Chem. 71 (1993) 1828–1833.
[17] C.D. Gabbutt, J.D. Hepworth, B.M. Heron, Dyes Pigments 42 (1999) 35–43.
[18] T. Yamaguchi, T. Tamaki, Y. Kawanishi, T. Seki, M. Sakuragi, J. Chem. Soc., Commun. (1990) 867–869.
[19] C. Miliani, A. Romani, G. Favaro, J. Phys. Org. Chem. 13 (2000) 141–150.
[20] X.D. Sun, M.G. Fan, X.J. Meng, E.T. Knobbe, J. Photochem. Photobiol. A: Chem. 102 (1997) 213–216.
[21] M. Fan, X. Sun, Y. Liang, Y. Zhao, Y. Ming, E.T. Knobbe, Mol. Cryst. Liq. Cryst. 298 (1997) 29–36.
[22] L.S. Kol'tsova, N.L. Zaichenko, A.I. Shiyonok, V.S. Marevtsev, Russ. Chem. Bull., Int. Ed. 50 (2001) 1214–1217.
[23] J. Zhou, Y. Li, Y. Tang, F. Zhao, X. Song, E. Li, J. Photochem. Photobiol. A: Chem. 90 (1995) 117–123.
[24] P.L. Gentili, M. Nocchetti, C. Miliani, G. Favaro, New. J. Chem. 28 (2004) 379–386.